

THE CRYSTAL STRUCTURE OF GLADIUSITE, $(\text{Fe}^{2+}, \text{Mg})_4\text{Fe}^{3+}_2(\text{PO}_4)(\text{OH})_{11}(\text{H}_2\text{O})$

ELENA SOKOLOVA[§] AND FRANK C. HAWTHORNE

Department of Geological Sciences, University of Manitoba, Winnipeg, Manitoba R3T 2N2, Canada

CATHERINE McCAMMON

Bayerisches Geoinstitut, Universität Bayreuth, D-95440 Bayreuth, Germany

RUSLAN P. LIFEROVICH

Institute of Geosciences, University of Oulu, PL 8000, FIN-90401 Oulu, Finland

ABSTRACT

The crystal structure of gladiusite, $(\text{Fe}^{2+}, \text{Mg})_4\text{Fe}^{3+}_2(\text{PO}_4)(\text{OH})_{11}(\text{H}_2\text{O})$, monoclinic, a 16.950 (2), b 11.650 (1), c 6.2660 (6) Å, β 90.000 (4)°, V 1237.3(4) Å³, space group $P2_1/n$, $Z = 2$, $D(\text{calc.}) = 3.08 \text{ g cm}^{-3}$, was solved by direct methods for a twinned crystal and refined to an R_1 index of 5.4% based on 1214 observed [$F_o > 4\sigma F$] unique reflections measured with MoK α X-radiation on a CCD diffractometer. There is one P site tetrahedrally coordinated by four O atoms. There are six distinct octahedrally coordinated M sites containing Fe^{3+} , Fe^{2+} , Mg and Mn^{2+} ; the octahedra are coordinated by O atoms, OH and H₂O groups. The ($M\varphi_6$) (φ = unspecified anion) octahedra each share two *trans* edges to form a rutile-like [$M\varphi_4$] chain along [001]. Pairs of chains, shifted relative to each other by a half-octahedron, link together through common edges to form a ribbon extending along c ; thus, each octahedron shares four edges with other octahedra. These ribbons are connected through common vertices of ($M\varphi_6$) octahedra into a framework with channels along the c axis. The (PO₄) tetrahedra share each of two vertices with three ($M\varphi_6$) octahedra, and the remaining two vertices are connected to octahedra through hydrogen bonds. There is a system of hydrogen bonds in the crystal structure of gladiusite ($D-A < 3.50$ Å), some of them bifurcated. The Mössbauer spectrum of gladiusite shows three doublets, two of which may be assigned to Fe^{2+} in octahedral coordination and one of which may be assigned to Fe^{3+} in octahedral coordination. The intensity ratios of the various doublets indicate that $\text{Fe}^{2+}/(\text{Fe}^{2+} + \text{Fe}^{3+}) = 0.49$.

Keywords: gladiusite, new mineral species, phosphate, crystal structure, twinning, Mössbauer spectroscopy.

SOMMAIRE

Nous avons résolu la structure cristalline d'un cristal maclé de gladiusite, $(\text{Fe}^{2+}, \text{Mg})_4\text{Fe}^{3+}_2(\text{PO}_4)(\text{OH})_{11}(\text{H}_2\text{O})$, monoclinique, a 16.950 (2), b 11.650 (1), c 6.2660 (6) Å, β 90.000 (4)°, V 1237.3(4) Å³, groupe spatial $P2_1/n$, $Z = 2$, $D(\text{calc.}) = 3.08 \text{ g cm}^{-3}$, par méthodes directes jusqu'à un résidu R_1 de 5.4% en utilisant 1214 réflexions uniques observées [$F_o > 4\sigma F$] et mesurées avec rayonnement MoK α et un diffractomètre CCD. La structure contient un site P à coordination tétraédrique avec quatre atomes d'oxygène, et six sites M à coordination octaédrique contenant Fe^{3+} , Fe^{2+} , Mg et Mn^{2+} . Les coins de ces octaèdres sont faits d'atomes d'oxygène et de groupes OH et H₂O. Les octaèdres ($M\varphi_6$) (φ : anion non spécifié) partagent dans chaque cas deux arêtes *trans* pour former une chaîne [$M\varphi_4$] le long de [001], semblable à celle dans le rutile. Des paires de telles chaînes, décalées d'un demi octaèdre l'une par rapport à l'autre, sont liées par partage d'arêtes communes pour former un ruban le long de c ; ainsi, chaque octaèdre partage quatre arêtes avec d'autres octaèdres. Ces rubans sont connectés par coins communs des octaèdres ($M\varphi_6$) pour former une trame avec canaux le long de l'axe c . Les tétraèdres (PO₄) partagent chacun de deux coins avec trois octaèdres ($M\varphi_6$), et les deux autres coins sont connectés à des octaèdres par liaisons hydrogène. Il y a un réseau de liaisons hydrogène dans la structure de la gladiusite ($D-A < 3.50$ Å), dans quelques cas avec bifurcation. Le spectre de Mössbauer de la gladiusite montre trois doublets, dont deux pourraient être dus au Fe^{2+} en coordination octaédrique; le troisième pourrait représenter le Fe^{3+} en coordination octaédrique. Les rapports d'intensité des divers doublets indiquent un rapport $\text{Fe}^{2+}/(\text{Fe}^{2+} + \text{Fe}^{3+})$ égal à 0.49.

(Traduit par la Rédaction)

Mots-clés: gladiusite, nouvelle espèce minérale, phosphate, structure cristalline, macle, spectre de Mössbauer.

[§] E-mail address: sokolova@ms.cc.umanitoba.ca

INTRODUCTION

Gladiusite, $(\text{Fe}^{2+}, \text{Mg})_4 \text{Fe}^{3+}_2 \text{Fe}^{3+}_2 (\text{PO}_4)_{11} (\text{H}_2\text{O})$, is a phosphate mineral from the Kovdor alkaline-ultrabasic complex, Kola Peninsula, Russia, recently described by Liferovich *et al.* (2000). It occurs in low-temperature hydrothermal assemblages related to the phosphorite-carbonatite complex (Figs. 1a, b), and is considered to form as a result of Fe released by hydrothermal leaching of primary pyrrhotite and P released during alteration of primary fluorapatite to secondary hydroxylapatite (Liferovich *et al.* 2000). The structure of gladiusite was solved and refined, and the Mössbauer spectrum was recorded, as part of the characterization of this mineral, particularly the derivation of the correct chemical formula; the results are presented here.

EXPERIMENTAL

Structure solution and refinement

A single crystal of gladiusite (Table 1) from the holotype specimen was attached to a glass fiber and mounted on a Siemens P4 automated four-circle diffractometer equipped with graphite-filtered $\text{MoK}\alpha$ X-radiation and a Smart 1K CCD detector. The intensities of 6761 reflections with $24 < h < 24$, $15 < k < 17$, $9 < l < 9$ were collected up to $60^\circ 2\theta$ using 30 s per frame, and an empirical absorption correction (SADABS, Sheldrick 1996) was applied. The refined unit-cell parameters were obtained from 2830 reflections with $I > 10\sigma I$.

The SHELXTL 5.03 system of programs was used for solution and refinement of the structure. Details of X-ray data collection and structure refinement are given



FIG. 1a. A cluster of gladiusite crystals in a vug in dolomite carbonatite.



FIG. 1b. Spherulites and clusters of gladiusite crystals on aggregate of fine-grained magnetite in a vug caused by the leaching of pyrrhotite.

TABLE 1. MISCELLANEOUS REFINEMENT DATA FOR GLADIUSITE

a (Å)	16.950(2)	Crystal size (mm)	0.004 x 0.004 x 0.016
b	11.650(1)	Radiation	MoK α
c	6.2660(6)	2 θ -range for data collection (°)	60.22
β (°)	90.000(4)	R (int)	0.0499
V (Å ³)	1237.3(4)	Reflections collected	6761
Space group	$P2_1/n$	Independent reflections $F_o > 4\sigma F$	1801 1214
Z	4	Refinement method	Full-matrix least squares on F^2 ; fixed weights proportional to $1/s(F_o^2)$
Absorption coefficient (mm ⁻¹)	6.00	Goodness of fit on F^2	0.998
$F(000)$	1140.0	Final R indices [$F_o > 4\sigma(F_o)$]	$R1 = 0.0540$
		R indices (all data)	$R1 = 0.0928$ $WR2 = 0.1270$ $Goof = 1.120$

in Table 1. Initially, we treated gladiusite as an orthorhombic phase with space-group symmetry $Pnma$ and unit-cell parameters a 16.950, b 11.650, c 3.133 Å. The structure was solved (by direct methods) on this basis and refined to an R -index of 5.9% for 784 unique observed reflections. However, inadequacies in several aspects of the structure refinement, particularly regarding the stereochemical details of the phosphate tetrahedra, suggested the presence of twinning, and twinning by rotation around a two-fold axis parallel to [001] was recognized for a structure with monoclinic symmetry, space-group symmetry $P2_1/n$ and unit-cell parameters $a_m = a_o$, $b_m = b_o$, $c_m = 2c_o$, $\beta = 90^\circ$. Two twinned components were introduced into the refinement, and full-matrix least-squares refinement of all positional variables, anisotropic-displacement parameters, site-scattering values for those sites occupied by Fe, Mg and Mn, and the volume ratio of the twin components, converged to an R -index of 5.4% for 1214 independent observed reflections. Final site coordinates and anisotropic-displacement parameters are given in Table 2, selected interatomic distances are listed in Table 3, and refined site-scattering values (in *epfu*: electrons per formula unit) are given in Table 4. Table 5 gives the bond-valence table for gladiusite, and a proposed hydrogen-bonding scheme is given in Table 6. Observed and calculated structure-factors may be obtained from The Depository of Unpublished Data, CISTI, National Research Council, Ottawa, Ontario K1A 0S2, Canada.

Electron-microprobe analysis

Subsequent to the collection of the X-ray intensity data, the crystal used for this purpose was embedded in epoxy, ground, polished, carbon-coated and analyzed with a Cameca SX-50 electron microprobe operating in wavelength-dispersion mode. Full details were given by Liferovich *et al.* (2000). The chemical composition is given in Table 7; the FeO and Fe₂O₃ contents were calculated from the Fe²⁺/(Fe²⁺ + Fe³⁺) ratio derived from the Mössbauer spectrum (Table 8). The unit formula was calculated on the basis of 16 anions with one H₂O and eleven OH groups per formula unit.

Mössbauer spectroscopy

Several needles of gladiusite were removed from the bulk sample and mounted in a hole 1 mm in diameter that had been drilled in a 10 μ m thick Pb foil; care was taken not to crush the needles. On observation under a binocular microscope, the sample consisted primarily of black needles, but there was also some greenish powder and reddish powder present. Care was used to avoid including the powder, but the presence of a small amount of this powder in the sample taken for Mössbauer spectroscopy cannot be ruled out. The effective thickness of the sample is estimated to be approximately 2 mg Fe/cm². A Mössbauer spectrum was collected at room temperature (293 K) using a

TABLE 2. FINAL ATOM POSITIONS AND DISPLACEMENT PARAMETERS FOR GLADIUSITE

	x	y	z	U_{eq}^*	U_{11}	U_{22}	U_{33}	U_{23}	U_{13}	U_{12}
M(1)	0.0742(2)	0.5653(3)	0.624(2)	0.0088(5)	0.0085(11)	0.0101(11)	0.0079(12)	-0.0019(19)	0.0082(13)	0.0005(12)
M(2)	0.0697(4)	0.5672(4)	0.124(2)	0.0088(5)	0.0085(11)	0.0101(11)	0.0079(12)	-0.0019(19)	0.0082(13)	0.0005(12)
M(3)	0.2382(2)	0.0034(3)	0.623(2)	0.0072(5)	0.0061(10)	0.0092(10)	0.0061(11)	0.0072(19)	-0.0009(12)	0.0006(11)
M(4)	0.2326(3)	0.0105(4)	0.118(2)	0.0072(5)	0.0061(10)	0.0092(10)	0.0061(11)	0.0072(19)	-0.0009(12)	0.0006(11)
M(5)	0.1152(2)	0.8388(3)	0.871(1)	0.0074(5)	0.0074(12)	0.0088(11)	0.0060(11)	0.0000(26)	0.0009(18)	0.0001(9)
M(6)	0.1098(5)	0.8448(8)	0.378(4)	0.0074(5)	0.0074(12)	0.0088(11)	0.0060(11)	0.0000(26)	0.0009(18)	0.0001(9)
P	-0.0593(2)	0.7281(3)	0.374(2)	0.0158(8)	0.0135(14)	0.0162(17)	0.0178(17)	-0.0176(40)	-0.0022(44)	0.0019(13)
O(1)(OH)	0.118(1)	0.9641(15)	0.636(7)	0.0117(13)	0.0144(23)	0.0120(26)	0.0087(26)	-0.0090(52)	0.0058(50)	0.0014(19)
O(2)(OH)	0.114(1)	0.957(2)	0.136(8)	0.0117(13)	0.0144(23)	0.0120(26)	0.0087(26)	-0.0090(52)	0.0058(50)	0.0014(19)
O(3)(OH)	0.229(1)	0.122(2)	0.871(6)	0.0149(21)	0.0150(21)	0.0144(31)	0.0154(53)	-0.0060(59)	-0.0093(62)	0.0022(21)
O(4)(OH)	0.229(1)	0.112(2)	0.396(5)	0.0149(21)	0.0150(21)	0.0144(31)	0.0154(53)	-0.0060(59)	-0.0093(62)	0.0022(21)
O(5)(OH)	0.1214(9)	0.728(2)	0.617(7)	0.0119(15)	0.0142(34)	0.0079(21)	0.0135(28)	-0.0053(54)	-0.0134(68)	0.0004(22)
O(6)(OH)	0.132(1)	0.726(2)	0.116(8)	0.0119(15)	0.0142(34)	0.0079(21)	0.0135(28)	-0.0053(54)	-0.0134(68)	0.0004(22)
O(7)(OH)	0.144(1)	0.495(2)	0.866(7)	0.0237(53)	0.0186(75)	0.0385(96)	0.0139(97)	-0.0324(117)	-0.0046(119)	0.0095(66)
O(8)(OH)	0.143(1)	0.507(2)	0.385(7)	0.0237(53)	0.0186(75)	0.0385(96)	0.0139(97)	-0.0324(117)	-0.0046(119)	0.0095(66)
O(9)(OH)	0.235(1)	0.879(2)	0.868(8)	0.0110(16)	0.0133(21)	0.0095(26)	0.0102(40)	-0.0036(53)	-0.0046(51)	0.0004(19)
O(10)(OH)	0.232(1)	0.886(2)	0.358(8)	0.0110(16)	0.0133(21)	0.0095(26)	0.0102(40)	-0.0036(53)	-0.0046(51)	0.0004(19)
O(11)	-0.0159(7)	0.8456(8)	0.392(5)	0.0137(21)	0.0115(42)	0.0226(33)	0.0069(40)	-0.0009(47)	-0.0101(54)	0.0006(29)
O(12)(W)	-0.0002(9)	0.834(1)	0.899(5)	0.0137(21)	0.0115(42)	0.0226(33)	0.0069(40)	-0.0009(47)	-0.0101(54)	0.0006(29)
O(13)(OH)	-0.0059(9)	0.589(1)	0.879(8)	0.0124(13)	0.0163(26)	0.0101(51)	0.0108(25)	0.0007(90)	0.0078(72)	0.0015(30)
O(14)	-0.0118(9)	0.615(1)	0.367(7)	0.0124(13)	0.0163(26)	0.0101(51)	0.0108(25)	0.0007(90)	0.0078(72)	0.0015(30)
O(15)	-0.1005(6)	0.737(1)	0.153(2)	0.0145(24)	0.0083(44)	0.0168(35)	0.0183(65)	0.0001(43)	0.0003(33)	0.0145(24)
O(16)	-0.1171(8)	0.725(1)	0.561(2)	0.0145(24)	0.0083(44)	0.0168(35)	0.0183(65)	0.0001(43)	0.0003(33)	0.0145(24)

$$* U_{eq} = (1/3)\sum_i U_{ij} a_i^* a_j^* a_i a_j$$

TABLE 3. SELECTED INTERATOMIC DISTANCES (Å) IN GLADIUSITE

M(1)-O(8)	2.02(3)	M(2)-O(13)	2.02(4)
M(1)-O(5)	2.05(2)	M(2)-O(13)'	2.12(2)
M(1)-O(7)	2.09(4)	M(2)-O(6)	2.13(2)
M(1)-O(13)	2.11(4)	M(2)-O(8)	2.17(4)
M(1)-O(14)	2.20(3)	M(2)-O(14)	2.17(4)
M(1)-O(14)'	<u>2.35(2)</u>	M(2)-O(7)	<u>2.21(4)</u>
<M(1)-O>	2.14	<M(2)-O>	2.14
M(3)-O(4)	1.91(3)	M(4)-O(3)	2.02(3)
M(3)-O(7)	2.00(2)	M(4)-O(10)	2.09(4)
M(3)-O(3)	2.09(3)	M(4)-O(4)	2.11(3)
M(3)-O(1)	2.09(2)	M(4)-O(8)	2.11(2)
M(3)-O(9)	2.11(4)	M(4)-O(2)	2.11(2)
M(3)-O(10)	<u>2.15(4)</u>	M(4)-O(9)	<u>2.19(4)</u>
<M(3)-O>	2.06	<M(4)-O>	2.11
M(5)-O(12)	1.97(2)	M(6)-O(2)	2.00(4)
M(5)-O(6)	2.04(4)	M(6)-O(5)	2.04(4)
M(5)-O(5)	2.05(4)	M(6)-O(11)	2.13(2)
M(5)-O(1)	2.08(4)	M(6)-O(10)	2.13(2)
M(5)-O(9)	2.09(2)	M(6)-O(1)	2.14(4)
M(5)-O(2)	<u>2.16(4)</u>	M(6)-O(6)	<u>2.18(4)</u>
<M(5)-O>	2.07	<M(6)-O>	2.10
P-O(16)	1.53(2)		
P-O(15)	1.55(1)		
P-O(14)	1.55(1)		
P-O(11)	<u>1.59(1)</u>		
<P-O>	1.55		

milliprobe spectrometer as described by McCammon *et al.* (1991). The data were fitted to three Lorentzian doublets (component doublets constrained to equal widths and areas), which was sufficient to account for all spectral absorption; the results are given in Table 8.

DISCUSSION

Mössbauer spectrum

The Mössbauer spectrum of gladiusite (Fig. 2) consists of three doublets that are sufficiently resolved that model-independent hyperfine parameters can be determined. Two doublets correspond to Fe²⁺, and the third corresponds to Fe³⁺. This is the minimum number of doublets required to fit the spectrum, but does not imply that there are only two Fe²⁺ sites in the structure. The line width of the Fe²⁺(I) doublet is relatively narrow, suggesting that it does correspond to either a single site in the structure, or to several sites with similar characteristics. In contrast, the large line-width of the Fe²⁺(II) doublet suggests that there may be more than one site contributing to this absorption, or that there is a large variation among different Fe²⁺(II) sites (*e.g.*, different next-nearest-neighbor environments, or variation in bond lengths). From the value of the center shifts, Fe²⁺(I) and Fe³⁺ likely correspond to octahedrally coordinated sites, whereas Fe²⁺(II) may indicate a site with

TABLE 8. MÖSSBAUER PARAMETERS* FOR THE SPECTRUM OF GLADIUSITE AT ROOM TEMPERATURE

	$^{57}\text{Fe}^{2+}$	$^{57}\text{Fe}^{2+}$	Fe^{3+}
Centre shift (mm/s)*	11.1(1)	1.19(3)	0.33(1)
Quad. split. (mm/s)	2.45(1)	1.39(8)	0.45(2)
FWHM (mm/s)	0.34(1)	0.58(7)	0.42(1)
Area fraction	0.34	0.15	0.51

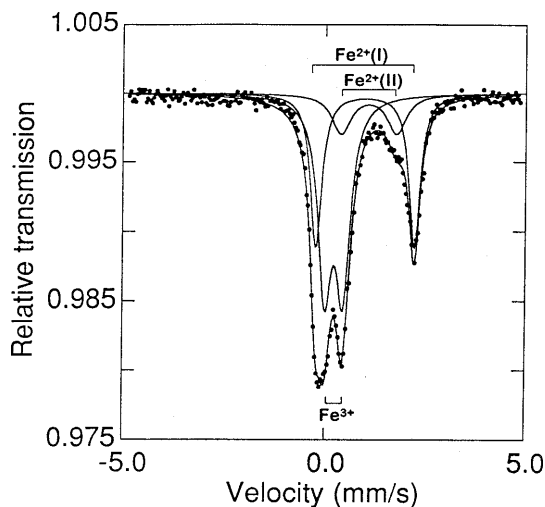
* relative to $\alpha\text{-Fe}$.

Fig. 2. Mössbauer spectrum of gladiusite at room temperature.

higher coordination. The relative areas give (to a first approximation) the relative abundance of each of the types of sites, and 51% of Fe occurs as Fe^{3+} (Table 8).

Cation polyhedra

There is one *P* site, occupied by P and coordinated by a tetrahedral array of O atoms with a $\langle P\text{-O} \rangle$ distance of 1.55 Å, reasonably close to the grand $\langle P\text{-O} \rangle$ distance of 1.537 Å given by Baur (1974).

There are six *M* sites, all coordinated by distorted octahedral arrays of O atoms with $\langle M\text{-O} \rangle$ distances in the range 2.06–2.14 Å; this range is in accord with the constituent cations at these sites, as indicated by the unit formula (Table 7). The total scattering at the *M* sites is 127.1 electrons per formula unit, *epfu* (Table 4), and the scattering from the *M* cations of the unit formula is 129.7 *epfu*. This agreement is reasonable, but results in 0.14 □ *pfu* at the *M* sites (Table 7). Omitting these vacancies and normalizing the sum of the M^{2+} cations to 4 *apfu* results in scattering from the *M* cations (as indicated from the unit formula) of 132.8 *epfu*, a difference of 5.7

epfu (= 4.5%). This difference is quite significant, and hence we presume that the vacancies are present at the *M* sites (Table 7). As a first step, we divide the scattering species into two types: Fe^* (= $\text{Fe}^{2+} + \text{Fe}^{3+} + \text{Mn}$) and Mg; the amount of Mn is sufficiently small that it can be considered together with Fe^{2+} . The site-scattering values indicate the scattering species (Fe^* and Mg) given in Table 4. Three of the sites [*M*(1), *M*(3) and *M*(5)] have only a minor amount of Mg (≤ 0.05 atoms per formula unit, *apfu*) present, as indicated by the site-scattering values; however, the very small amounts of Mg at these sites may well be spurious, and we consider *M*(1), *M*(3) and *M*(5) completely occupied by Fe^* . The two remaining sites [*M*(2) and *M*(4)] are occupied by $\sim 0.50 \text{ Fe}^*$ and $\sim 0.50 \text{ Mg}$.

Thus far, 0.95 Mg has been assigned to the *M*(1)–*M*(5) sites, leaving 0.66 Mg to be assigned to *M*(6). However, the refined scattering at *M*(6) is 12 *epfu*, essentially equivalent to 2.00 Mg *apfu*. Thus we have no choice but to assign the observed amount of vacancy, 0.14 □ *pfu* to *M*(6). The Mg and Fe^* assigned to *M*(6) were adjusted to produce the observed scattering (Table 4). At this stage, the scattering species Fe^* , Mg and □ have been assigned to the *M*(1)–*M*(6) sites.

Next, we need to resolve Fe^* into its component species Fe^{2+} , Fe^{3+} and Mn. The *M*(1), *M*(3) and *M*(5) sites contain only Fe^* , and hence the Fe^{2+} and Fe^{3+} contents at these sites can be calculated from the hard-sphere model, using the empirical radii for $^{56}\text{Fe}^{2+}$ (0.78 Å) and $^{56}\text{Fe}^{3+}$ (0.645 Å) (Shannon 1976). The resultant values are given in Table 4. Mn^{2+} is quite large (0.83 Å), and hence it must be placed at *M*(2), and the Fe^* at *M*(2) must be assigned as Fe^{2+} in order to reproduce the observed $\langle M(2)\text{-O} \rangle$ distance, 2.14 Å. The Fe^{2+} and Fe^{3+} contents of *M*(4) were also calculated from the hard-sphere model. Similarly, the Fe^* at *M*(6) needs to be Fe^{2+} in order to reproduce the observed $\langle M(6)\text{-O} \rangle$ distance (assuming a radius for the vacancy intermediate between that of ^{56}Mg and ^{56}Fe).

At this stage, the total Fe and Mg contents agree reasonably well with the unit formula calculated from the chemical composition (Table 7). However, the $\text{Fe}^{2+}/\text{Fe}^{3+}$ ratio was wrong. This ratio is fixed by the electroneutrality principle, and hence our assumption of a hard-sphere model is not quite correct; our relative site-populations are good, but our absolute values need adjustment to produce the correct Fe^{2+} and Fe^{3+} contents. Thus the Fe^{2+} and Fe^{3+} values were adjusted accordingly, and the resultant site-populations are shown in Table 4.

Structure topology

The *M*(1) and *M*(2) octahedra alternate and share *trans* edges to form an $[M\phi_4]$ chain that extends in the *c* direction. Pairs of these chains meld by sharing edges to form an $[M\phi_3]$ ribbon along *c* (Fig. 3). In a similar fashion, *M*(3) + *M*(4) and *M*(5) + *M*(6) each form $[M\phi_4]$

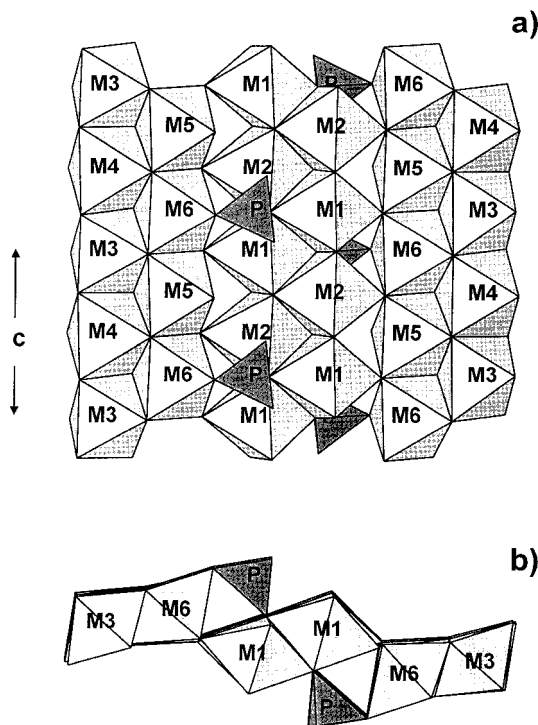


FIG. 3. A fragment of the structure of gladiusite (a) viewed orthogonal to the c axis down a non-rational direction that is approximately perpendicular to the triplet of $[MT\phi_4]$ ribbons in the structure; (b) projected down the c axis; octahedra and tetrahedra are labeled.

trans chains that link to form an $[M\phi_3]$ ribbon along c . These ribbons link by sharing corners between octahedra: one-connected vertices of the $M[1+2]$ ribbon link to the *trans* shared edges of the $M[3+4+5+6]$ ribbon on each side of the central $M[1+2]$ ribbon. The ribbons are further linked through phosphate groups that share one vertex with each ribbon. The resulting unit, a decorated stepped ribbon, is illustrated in Figures 3a and b.

Figure 4 shows how the complex ribbons of octahedra and tetrahedra in Figure 3 are linked together. The ribbons are inclined at $\sim 45^\circ$ to the a axis and are repeated by the b translation to form a row of parallel ribbons centered on $c \approx 0$, and another row centered on $c \approx \frac{1}{2}$ and with the opposite inclination to the a axis. Adjacent rows of ribbons merge by sharing octahedron vertices (Fig. 4). The terminal-octahedron vertices of each ribbon link to the central-octahedron vertices of ribbons in adjacent rows. The resultant structure is a heteropolyhedral framework with extensive development of hydrogen bonds between octahedron–octahedron and octahedron–tetrahedron vertices (Fig. 4).

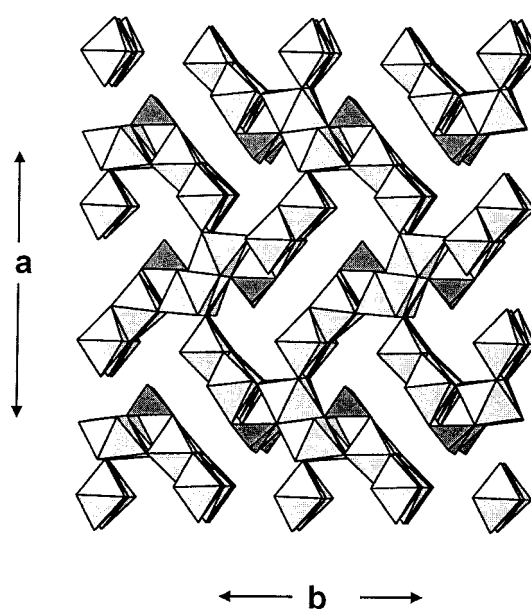


FIG. 4. The crystal structure of gladiusite projected down a direction a few degrees away from $[001]$; legend as in Figure 3.

Hydrogen bonding

All O atoms not bonded to P are (OH) or (H_2O) groups, and incident bond-valence sums (Table 5) indicate that three of the four anions bonded to P must be hydrogen-bond acceptors. Hence there must be an extensive hydrogen-bond network in gladiusite. No H positions were detected in the final difference-Fourier maps, but a hydrogen-bond arrangement was derived from examination of local stereochemistry and the bond-valence requirements of the anions in the structure (Table 5, central Σ column).

If we write the formula of gladiusite as $Fe^{3+}_2(Fe^{2+}, Mg)_4P\phi_{16}$, where ϕ is an unspecified anion, the sum of the positive charges is 19^+ and the charge of the 16 anions must be 19^- . Hence there must be 13 H atoms in the formula of gladiusite. The following anions have incident bond-valence sums of ~ 1.0 *vu* (valence units): O(1), O(2), O(3), O(4), O(6), O(8), O(9), O(10) and O(13); these must be (OH) groups. The O(14) anion has an incident bond-valence sum of 2.0 *vu* and must be an O^{2-} anion. The O(12) anion (Table 5) has an incident bond-valence of 0.56 *vu*, neglecting any H atoms, and hence must be an (H_2O) group. This leaves $13 - 11 = 2$ H atoms to be assigned to one or more of the following anions: O(5): 1.31; O(7): 1.20; O(11): 1.48; O(5): 1.20; O(16): 1.27 *vu*. If O(11) were an (OH) group, the associated H atom would have to be involved in a symmetri-

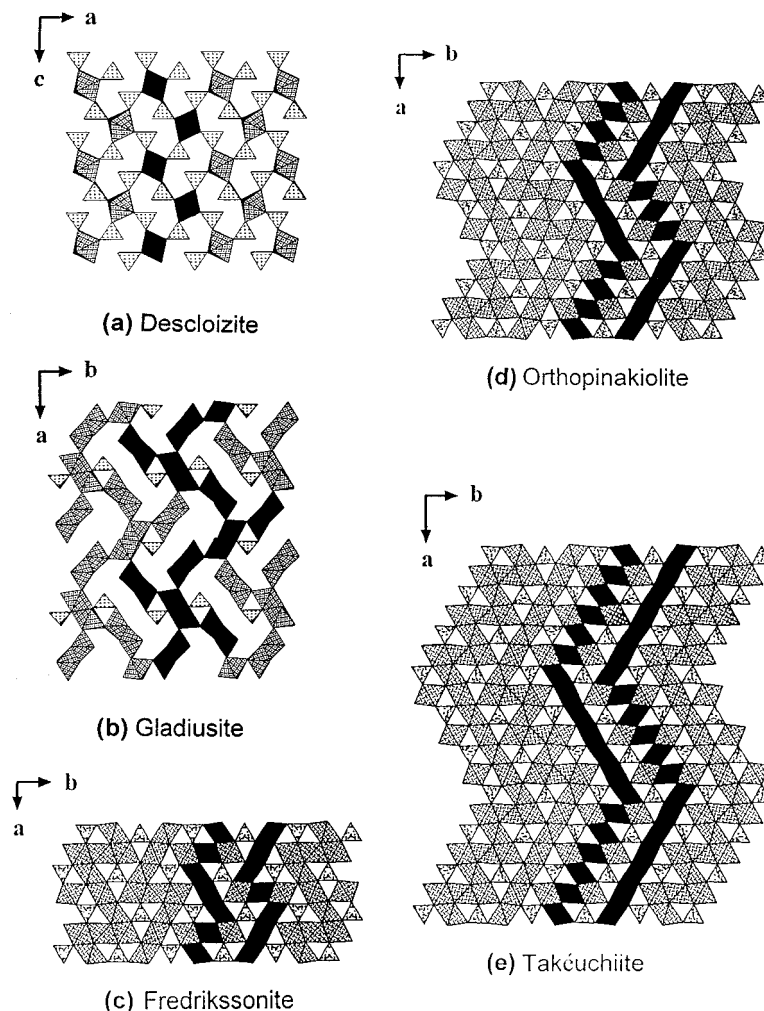
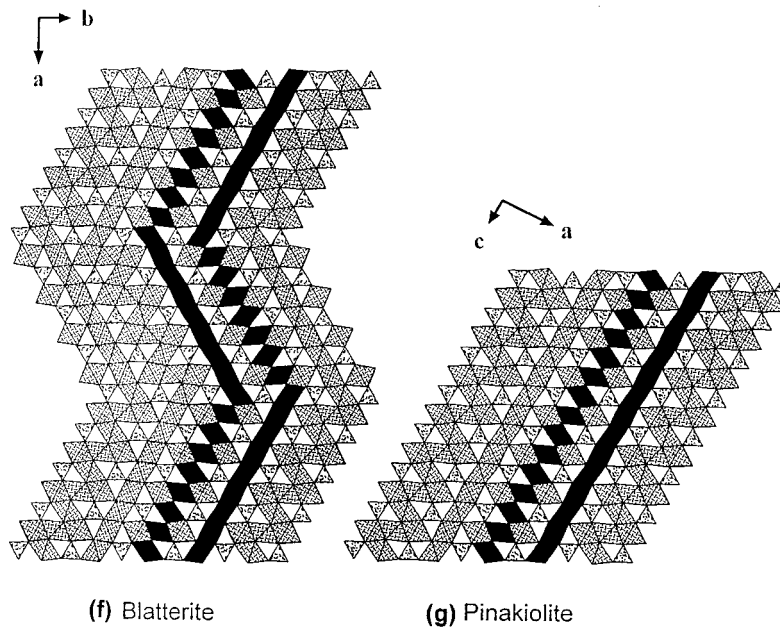


FIG. 5. Various $[M\phi_4]$ -derivative structures projected down the chain axis: (a) descloizite, (b) gladiusite, (c) fredrikssonite, (d) orthopinakiolite, (e) takéuchiite, (f) blatterite, (g) pinakiolite. The ribbons and linking octahedra are shaded black for emphasis.

cal hydrogen-bond; the infrared spectrum of gladiusite (Liferovich *et al.* 2000) shows that a symmetrical hydrogen-bond is *not* present, and hence O(11) must be an O^{2-} anion that is an acceptor for two or more hydrogen bonds. We are left with four anions, O(5), O(7), O(15) and O(16), each with an incident bond-valence sum of $\sim 1.25 \text{ vu}$; thus, two of these anions must be (OH) groups and two of them must be O^{2-} anions that are acceptor anions for four or five hydrogen bonds (*e.g.*, $1.25 + 4 \times 0.20 = 2.05 \text{ vu}$). The O(5) and O(7) anions are each bonded to three octahedrally coordinated cations, and the space around these anions is not sufficient for 4 or 5 H atoms to be close enough to form hydrogen bonds. Conversely, O(15) and O(16) are bonded to one cation

only (and that in tetrahedral coordination), and hence there is ample space for 4 or 5 H atoms to form hydrogen bonds with each of these two anions as acceptors. Thus $O(5) = O(7) = (\text{OH})$ and $O(15) = O(16) = O^{2-}$. Hydrogen bonds were identified by short *D* (Donor) to *A* (Acceptor) distances, where *D* and *A* are ligands for different cations; the *D*-*A* distances are given in Table 6, where the H atoms are numbered such that O(*n*) is the donor involving H(*n*) [except for O(12), which is an (H_2O) group involving H(11) and H(12)]. The resultant bond-valence arrangement is shown in Table 5. Note that the phosphate ligands O(11), O(15) and O(16) act as acceptors for 3, 4 and 5 hydrogen-bonds, respectively.



Related structures

The key motif in the structure of gladiusite is the $[MT\varphi_4]$ chain of edge-sharing octahedra. This is a common motif in a wide variety of oxysalt structures, and is usually decorated by tetrahedral oxyanions in a staggered fashion along its length. It occurs as isolated chains in the linarite-group minerals (*e.g.*, linarite, $Pb^{2+}[Cu^{2+}(SO_4)(OH)_2]$, Bachmann & Zemann 1961), the brackebuschite-group minerals (*e.g.*, brackebuschite, $Pb^{2+}[Mn^{2+}(VO_4)_2(H_2O)]$, Foley & Hughes 1997), the fornacite-group minerals (*e.g.*, fornacite, $Pb^{2+}[Cu^{2+}(AsO_4)(CrO_4)(OH)]$, Cocco *et al.* 1967), and the vauquelinite-group minerals (*e.g.*, vauquelinite, $Pb^{2+}[Cu^{2+}(PO_4)(CrO_4)(OH)]$, Fanfani & Zanazzi 1968). The decorated chain can polymerize as octahedron–tetrahedron-linked heteropolyhedral sheets in the tsumcorite-group minerals (*e.g.*, tsumcorite, $Pb^{2+}[ZnFe^{3+}(AsO_4)(H_2O)(OH)]$, Krause *et al.* 1998) and the bermanite-group minerals (*e.g.*, bermanite, $Mn^{2+}[Mn^{3+}(PO_4)(OH)_2](H_2O)_4$, Kampf & Moore 1976). The chain can also polymerize to form octahedron–tetrahedron-linked heteropolyhedral frameworks as in the descloizite-group minerals (*e.g.*, descloizite, $Pb^{2+}[Zn(VO_4)(OH)]$, Hawthorne & Faggiani 1979), the conicalcite-group minerals (*e.g.*, conicalcite, $Ca^{2+}[Cu^{2+}(AsO_4)(OH)]$, Qurashi & Barnes 1963), and numerous silicate minerals such as lawsonite ($Ca[Al_2(Si_2O_7)(OH)_2](H_2O)$, Comodi & Zanazzi 1996), pumpellyite ($Ca_2[Al_2(Al,Mg)(SiO_4)(Si_2O_7)(OH)_2(OH,H_2O)]$, Galli & Alberti 1969), and ardenite ($\{Mn,Ca\}_4[Al_4(Mg,Al)_2(SiO_4)_2(Si_3O_{10})(\{As,V\}O_4)(OH)_6]$, Donnay & Allmann 1968).

Perhaps the simplest of the framework structures is that of descloizite, $Pb^{2+}[Zn(VO_4)(OH)]$, in which $[ZnO_3(OH)]$ chains extend along $[010]$ and are cross-linked into a framework by (VO_4) tetrahedra (Fig. 5a). In projection (Fig. 4a), corner-linked octahedra and tetrahedra form an 8^4 net with octahedra and tetrahedra at alternate vertices of the net. These $[MT\varphi_4]$ chains can also polymerize directly by sharing octahedron vertices. In gladiusite, the $[MT\varphi_4]$ chains link into pairs by sharing edges to form ribbons that extend along the c direction (Fig. 3a). These ribbons polymerize further by sharing octahedron corners and by linking *via* tetrahedron vertices (Fig. 5b). There is a complete family of structures in which the $[MT\varphi_4]$ chains polymerize directly to form ribbons of different widths. Of particular elegance are the structures of the zig-zag borate minerals (Cooper & Hawthorne 1998), which consist of ribbons of octahedra an odd number of $[M\varphi_4]$ chains wide that are linked by (BO_3) triangles and other octahedra. Fredrikssonite, $[Mg_2Mn^{3+}(BO_3)_2]$ Burns *et al.* (1994), has ribbons that are three octahedra wide (Fig. 5c); orthopinakiolite, $[Mn^{3+}_7(\{Mn^{2+},Mg\}_xFe^{3+}_y\Box_{(y-1)/2})_{\Sigma 17}(BO_3)_8O_{16}]$, Takéuchi *et al.* (1978), has ribbons that are five octahedra wide (Fig. 5d); takéuchiite, $[Mn^{3+}_{11}(\{Mn^{2+},Mg\}_xFe^{3+}_y\Box_{(y-1)/2})_{\Sigma 25}(BO_3)_{12}O_{24}]$, Norrestam & Bovin (1987), has ribbons that are seven octahedra wide (Fig. 5e); blatterite, $[Sb^{5+}_3Mn^{3+}_9(\{Mn^{2+},Mg\}_xFe^{3+}_y\Box_{(1+y)/2})_{\Sigma 36}(BO_3)_{16}O_{32}]$, Cooper & Hawthorne (1998), has ribbons that are nine octahedra wide; pinakiolite, $[(Mg,Mn^{2+})_2Mn^{3+}(BO_3)_2]$, Moore & Araki (1974), has sheets of octahedra, essentially ribbons an infinite number of octahedra wide, that are cross-linked

by (BO₃) triangles and other octahedra. Thus we see a wide variety of heteropolyhedral frameworks formed from ribbons of polymerized [MTφ₄] chains.

ACKNOWLEDGEMENTS

We thank Sergey V. Krivovichev, Don R. Peacor and Associate Editor Peter C. Burns for their comments on this paper. This work was supported by a NATO grant to EVS and Barbara L. Sherriff and by NSERC Major Facilities Access, Major Equipment and Research grants to FCH. Mr. M.A. Bogomolov took Figure 1b.

REFERENCES

- BACHMANN, H.G. & ZEMANN, J. (1961): Die Kristallstruktur von Linarit, PbCuSO₄(OH)₂. *Acta Crystallogr.* **14**, 747-753.
- BAUR, W.H. (1974): The geometry of polyhedral distortions. Predictive relationships for the phosphate group. *Acta Crystallogr.* **B30**, 1195-1215.
- BROWN, I.D. & ALTERMATT, D. (1985): Bond-valence parameters obtained from a systematic analysis of the inorganic crystal structure database. *Acta Crystallogr.* **B41**, 244-247.
- BURNS, P.C., COOPER, M.A. & HAWTHORNE, F.C. (1994): Jahn-Teller distorted Mn³⁺O₆ octahedra in fredrikssonite, the fourth polymorph of Mg₂Mn³⁺(BO₃)O₂. *Can. Mineral.* **32**, 397-403.
- COCCO, G., FANFANI, L. & ZANAZZI, P.F. (1967): The crystal structure of fornacite. *Z. Kristallogr.* **124**, 385-397.
- COMODI, P. & ZANAZZI, P.F. (1996): Effects of temperature and pressure on the structure of lawsonite. *Am. Mineral.* **81**, 833-841.
- COOPER, M.A. & HAWTHORNE, F.C. (1998): The crystal structure of blatterite, Sb⁵⁺₃(Mn³⁺, Fe³⁺)₉(Mn²⁺, Mg)₃₅(BO₃)₁₆O₃₂, and structural hierarchy in Mn³⁺-bearing zigzag borates. *Can. Mineral.* **36**, 1171-1193.
- DONNAY, G. & ALLMANN, R. (1968): Si₃O₁₀ groups in the crystal structure of ardenneite. *Acta Crystallogr.* **B24**, 845-855.
- FANFANI, L. & ZANAZZI, P.F. (1968): The crystal structure of vauquelinite and the relationship to fornacite. *Z. Kristallogr.* **126**, 433-443.
- FOLEY, J.A., HUGHES, J.M. & LANGE, D. (1997): The atomic arrangement of brackebuschite, redefined as Pb₂(Mn³⁺, Fe³⁺)(VO₄)₂(OH), and comments on Mn³⁺ octahedra. *Can. Mineral.* **35**, 1027-1033.
- GALLI, E. & ALBERTI, A. (1969): On the crystal structure of pumpellyite. *Acta Crystallogr.* **B25** 2276-2281.
- HAWTHORNE, F.C. & FAGGIANI, R. (1979): Refinement of the structure of descloizite. *Acta Crystallogr.* **B35**, 717-720.
- KAMPF, A.R. & MOORE, P.B. (1976): The crystal structure of bermanite, a hydrated manganese phosphate. *Am. Mineral.* **61**, 1241-1248.
- KRAUSE, W., BELENDORFF, K., BERNHARDT, H.-J., McCAMMON, C., EFFENBERGER, H. & MIKENDA, W. (1998): Crystal chemistry of the tsumcorite-group minerals. New data on ferrilotharmeyerite, tsumcorite, thometzekite, mounanaite, helmutwinklerite, and a redefinition of gartrellite. *Eur. J. Mineral.* **10**, 179-206.
- LIFEROVICH, R.P., SOKOLOVA, E.V., HAWTHORNE, F.C., LAAJOKI, K.V.O., GEHÖR, S., PAKHOMOVSKY, Y.A.A. & SOROKHTINA, N.V. (2000): Gladiusite, Fe³⁺₂(Fe²⁺, Mg)₄(PO₄)(OH)₁₁(H₂O), a new hydrothermal mineral species from the phoscorite-carbonatite complex, Kovdor Complex, Kola Peninsula, Russia. *Can. Mineral.* **38**, 1477-1485.
- McCAMMON, C.A., CHASKAR, V. & RICHARDS, G.G. (1991): A technique for spatially resolved Mössbauer spectroscopy applied to quenched metallurgical slags. *Meas. Sci. Technol.* **2**, 657-662.
- MOORE, P.B. & ARAKI, T. (1974): Pinakiolite, Mg₂Mn³⁺O₂[BO₃]; warwickite, Mg(Mg_{0.5}Ti_{0.5}O)[BO₃]; wightmanite, Mg₅(O)(OH)₅[BO₃]•nH₂O: crystal chemistry of complex 3 Å wallpaper structures. *Am. Mineral.* **59**, 985-1004.
- NORRESTAM, R. & BOVIN, J.-O. (1987): The crystal structure of takéuchiite, Mg_{1.71}Mn_{1.29}BO₅, a combined single crystal X-ray and HRTEM study. *Z. Kristallogr.* **181**, 135-149.
- QURASHI, M.M. & BARNES W.H. (1963): The structures of the minerals of the descloizite and adelite group. IV. Descloizite and conichalcite (part 2). The structure of conichalcite. *Can. Mineral.* **7**, 561-577.
- SHANNON, R.D. (1976): Revised effective ionic radii and systematic studies of interatomic distances in halides and chalcogenides. *Acta Crystallogr.* **A32**, 751-767.
- SHELDRIK, G.M. (1996): *SADABS User Guide*. University of Göttingen, Göttingen, Germany.
- TAKÉUCHI, Y. HAGA, N., KATO, T. & MIURA, Y. (1978): Orthopinakiolite, Me_{2.95}O₂[BO₃]: its crystal structure and relationship to pinakiolite, Me_{2.90}O₂[BO₃]. *Can. Mineral.* **16**, 475-485.

Received October 9, 2000, revised manuscript accepted July 10, 2001.